Molecular Cancer Research

Abemaciclib Is Effective Against Pancreatic Cancer Cells and Synergizes with HuR and YAP1 Inhibition

Teena Dhir[1], Christopher W. Schultz[1], Aditi Jain[1], Samantha Z. Brown[1], Alex Haber[1], Austin Goetz[1], Chunhua Xi[2], Gloria H. Su[2], Liang Xu[3], James Posey III[1], Wei Jiang[1], Charles J. Yeo[1], Talia Golan[4,5], Michael J. Pishvaian[6], and Jonathan R. Brody[1]

Abstract

Mutation or promoter hypermethylation of *CDKN2A* is found in over 90% of pancreatic ductal adenocarcinomas (PDAC) and leads to loss of function of cell-cycle inhibitors p16 (INK4A) and p14 (ARF) resulting in unchecked proliferation. The CDK4/6 inhibitor, abemaciclib, has nanomolar IC_{50}s in PDAC cell lines and decreases growth through inhibition of phospho-Rb (pRb), G_1 cell-cycle arrest, apoptosis, and the senescent phenotype detected with β-galactosidase staining and relevant mRNA elevations. Daily abemaciclib treatments in mouse PDAC xenograft studies were safe and demonstrated a 3.2-fold decrease in tumor volume compared with no treatment ($P < 0.0001$) accompanying a decrease in both pRb and Ki67. We determined that inhibitors of HuR (*ELAVL1*), a prosurvival mRNA stability factor that regulates cyclin D1, and an inhibitor of Yes-Associated Protein 1 (YAP1), a pro-oncogenic, transcriptional coactivator important for CDK6 and cyclin D1, were both synergistic with abemaciclib. Accordingly, siRNA oligonucleotides targeted against HuR, YAP1, and their common target cyclin D1, validated the synergy studies. In addition, we have seen increased sensitivity to abemaciclib in a PDAC cell line that harbors a loss of the *ELAVL1* gene via CRISP-Cas9 technology. As an *in vitro* model for resistance, we investigated the effects of long-term abemaciclib exposure. PDAC cells chronically cultured with abemaciclib displayed a reduction in cellular growth rates (GR) and coresistance to gemcitabine and 5-fluorouracil (5-FU), but not to HuR or YAP1 inhibitors as compared with no treatment controls. We believe that our data provide compelling preclinical evidence for an abemaciclib combination–based clinical trial in patients with PDAC.

Implications: Our data suggest that abemaciclib may be therapeutically relevant for the treatment in PDAC, especially as part of a combination regimen inhibiting YAP1 or HuR.

Introduction

Pancreatic ductal adenocarcinoma (PDAC) is one of the most aggressive solid tumors. (1, 2) Currently, the only curative option is surgery, but most patients present with inoperable disease. (3). In the metastatic setting, the standard of care is a combination of nontargeted chemotherapies, FOLFIRINOX (folinic acid, 5-fluorouracil, irinotecan, oxaliplatin) or gemcitabine plus nab-paclitaxel (4, 5). While these regimens are more effective than the previous standard of care of gemcitabine alone, they only increase median survival by a few months (6). These statistics highlight the need for new and targeted therapies for the treatment of PDAC.

CDKN2A encodes the cell-cycle inhibitor proteins p16(INK4A) and the p14(ARF; ref. 7). Loss of *CDKN2A* due to the gene mutation or promoter hypermethylation can be found in 90%–98% of PDAC cells (8). *CDKN2A* is an endogenous inhibitor of cell-cycle progression which, when activated, leads to a G_1 cell-cycle arrest through the inhibition of CDK4/6 (9). In dividing cells, the presence of growth factors or other progrowth signals leads to an increase in the transcription of cyclin D1 (10). Cyclin D1 can then bind and activate CDK4/6 to monophosphorylate and partially inactivate Rb early in the G_1 phase of the cell cycle (11). The Rb–E2F complex is an important transcriptional repressor of DNA synthesis, and its inactivation is necessary for the progression to S-phase. Inactivation of Rb leads to the release of the E2F 1–3 transcription factors (7, 12), and upon release, there is a transcriptional upregulation of target cell-cycle genes such as cyclin E and cyclin A (13), allowing for progression of the cell cycle into S-phase (14). As described above, in PDAC, loss of p16 leads to unchecked cellular division and disruption of the G_1–S checkpoints (15). When p16 is silenced, Rb remains nonfunctional as a regulator allowing for unchecked proliferation.

[1]Department of Surgery, Jefferson Pancreas, Biliary and Related Cancer Center, Thomas Jefferson University, Philadelphia, Pennsylvania. [2]The Department of Pathology & Cell Biology, Columbia University Medical Center, New York, New York. [3]Department of Molecular Biosciences, University of Kansas, Lawrence, Kansas. [4]Oncology institute, Chaim Sheba Medical Center, Tel Aviv, Israel. [5]Sackler Faculty of Medicine, Tel Aviv University, Tel Aviv, Israel. [6]MD Anderson Cancer Center, Houston, Texas.

Note: Supplementary data for this article are available at Molecular Cancer Research Online (http://mcr.aacrjournals.org/).

T. Dhir and C.W. Schultz contributed equally to this article.

Corresponding Author: Jonathan R. Brody, Thomas Jefferson University, 1015 Walnut Street, Curtis 618, Philadelphia, PA 19107. Phone: 215-955-2693; Fax: 215-923-6609; E-mail: jonathan.brody@jefferson.edu

Mol Cancer Res 2019;17:2029–41

doi: 10.1158/1541-7786.MCR-19-0589

While the p16 pathway is frequently disrupted in PDAC, Rb is commonly preserved in PDAC and the presence of pRb is an important predictor of response for CDK4/6 inhibitors (16, 17). As a strong premise for this study, others have demonstrated and advocated for the use of CDK4/6 inhibitors for the treatment of PDAC (2, 18, 19). To underscore this work, there is currently a phase Ib trial studying the effects of palbociclib with nab-paclitaxel in patients with metastatic pancreatic cancer (NCT02501902). In addition, the CDK4/6 inhibitor abemaciclib (LY2835219) is currently being investigated in a phase II trial, as a solo agent, and in combination with a PI3K inhibitor in patients with metastatic pancreatic cancer (NCT02981342). In regards to this study, abemaciclib has been described as a more selective inhibitor of CDK4/6 (20, 21), is FDA-approved for hormone receptor–positive breast cancer (14, 22), and is currently being tested for efficacy in lung cancer (22), esophageal cancer (23), and some other soft-tissue cancers (24), yet has limited preclinical evaluation in PDAC. Herein, we evaluate the efficacy of abemaciclib in preclinical PDAC models *in vitro* and *in vivo* and explore its mechanism of action, and screened for potential synergistic combinations.

Materials and Methods

In vitro

Cell lines and cell culture conditions (including PDXs). Human pancreatic cancer cell lines were purchased from the ATCC, confirmed negative for *Mycoplasma* contamination and validated using short tandem repeat profiling. All cells were cultured in DMEM supplemented with 10% FBS, antibiotics and L-glutamine. Patient-derived cell lines (PDX) were obtained from Dr. Talia Golan (The Chaim Sheba Medical Center at Tel HaShomer, Tel Aviv, Israel; ref. 25). PDX cell lines were cultured in RPMI supplemented with 10% FBS, antibiotics and L-glutamine. Mia PaCa2 "chronic" abemaciclib therapy lines were created by treating cell lines with increasing concentration of abemaciclib over 10 months and resistance testing was performed monthly using Pico Green assay to calculate IC_{50}/GR_{50}. All cell lines used in experiments were under passage 20, except for the resistant lines. 3D mouse organoids were generated from previously reported mouse models of PDAC, KPC, and PKP (26).

Chemical compounds. Most compounds used in this study were purchased from MedChem Express and Sigma-Aldrich. CMLD-2 was purchased from Millipore Sigma (catalog# 538339), and CA3 was purchased from Selleckchem (catalog# S8661). Abemaciclib, gemcitabine, and palbociclib were diluted in water to a 10 mmol/L stock concentration and stored at −20°C until use. Paclitaxel, CMLD2, pyrvinium pamoate, verteporfin, and CA3 were diluted in DMSO to a 10 mmol/L stock concentration and stored at −20°C/−80°C until use.

IC_{50}, GR_{50}, cell proliferation assay, and colony formation assay. Assessment of cellular viability and calculation of IC_{50} were performed using a Pico Green assay. Cells were seeded at 1,000 cells/well (Mia PaCa2) or 2,000 cells/well (Panc-1, HS 766T) in a 96-well plate and treated with drug for 5 days. Upon collection Pico Green (Thermo Fisher Scientific, catalog #P7581) was used as per manufacturer's instructions. Fluorescence (504 nm/531 nm) was determined using Promega GloMax machine. For cell lines with different proliferation and doubling times, we calculated growth rate inhibition (GR) and GR_{50} values using a published and validated GR calculator (http://www.grcalculator.org/grtutorial/Home.html; ref. 27).

For mouse organoid experiments, assessment of cellular viability was done using CellTiter Glo protocol (Promega, catalog# G7570). Cells were seeded at 1,500 cells/well in a 96-well plate and treated with drug for 5 days. At collection day, CellTiter Glo reagent was added directly to the wells, mixed for 10 minutes and incubated for 10 minutes. Luminescence was quantified using a Promega GloMax.

For colony-forming experiments, cells were seeded at 800 or 1,500 (Mia PaCa2), 2,000 (Panc-1), or 3,000 (HS 766T) cells/well respectively in a 6-well plate. Drug was replenished every 3 days for 10 days total. Colonies were fixed with 80% methanol and stained with 0.5% crystal violet/ 25% methanol solutions for 10 minutes each. Colonies were counted manually or using ImageJ software and graphed using Prism (version 7.03).

BrdU/cell-cycle analysis. Cells were treated with abemaciclib for 72 hours and upon collection were incubated with 10 μmol/L BrdU (Sigma, #B5002) for 1 hour prior and then fixed in ice-cold 70% ethanol. Cells were washed and incubated in 2 mol/L HCl for 1 hour to denature DNA. After washing, HCl was neutralized with 0.1 mol/L sodium borate (pH 8.5) for 10 minutes. Cells were stained with anti-BrdU FITC-conjugated antibody (Thermo Fisher Scientific, #11-5071-42) for 1 hour in the dark, washed, and stained with propidium iodide (PI) for 10 minutes. Samples were run using BD Celesta machine and data were analyzed using FlowJo (version 10) software.

Senescence assay. Cells were seeded at 3,000 cells/well in 24-well plates with glass coverslips inlay and treated with water or 0.5 μmol/L abemaciclib or H_2O_2 at 10 μmol/L, 100 μmol/L, or 500 μmol/L and collected at various days for detection of β-galactosidase (β-gal) using manufacturer's kit (Cell Signaling Technology, #9860). After treatment, cells were washed with PBS, fixed, permeabilized stained with β-gal, and mounted/stained with DAPI (Invitrogen/Thermo Fisher Scientific, #P36931) on a glass slide and imaged using Leica DM4B.

Reactive oxygen species assay. ROS assay was performed using DCFDA/H2DCFD Cellular ROS Detection Assay Kit (Abcam, catalog# ab113851). Cells were seeded at 3,000 cells/well and treated with water or 0.5 μmol/L abemaciclib or H_2O_2 at 10 μmol/L, 100 μmol/L, or 500 μmol/L. Upon collection samples were collected per kit protocol and fluorescence (485 nm/535 nm) was determined using a Promega GloMax.

Caspase 3/7 detection assay. Cells were seeded at 3,000 cells/well in 24-well plates. Upon collection the caspase 3/7 live stain was added (Thermo Fisher Scientific, #R37111) 1 drop per 0.5 mL of media was added and incubated for 1 hour. GFP and brightfield images were taken using the Evos FL cell imaging system.

Apoptosis assay. Annexin V/PI staining was performed using a flow cytometry kit (Thermo Fisher Scientific, # V13242). Changes in complexity and morphology of cells treated with water or 0.5 μmol/L abemaciclib after three days of treatment was monitored by forward and side scatter (FSC-A, SSC-A) measurements using BD Celesta machine. All events were gated excluding debris with a

minimum of 10,000 cells analyzed per sample. Data were analyzed using FlowJo software.

Western blot, IHC, and antibodies. Western blot and RNA immunoprecipitation assays were performed as described previously (28). For IHC, phospho-Rb, total Rb, Ki67, and TUNEL stainings were performed on 10% paraffin-embedded tumor slides as per the manufacturer's protocol and imaged using Leica florescence microscope at 20× and 40× magnifications. IHC staining was performed by our pathology department, by W. Jiang and R. O'Neill, at Thomas Jefferson University (Philadelphia, PA).

For protein evaluation by Western blot analysis, the following primary antibodies were used: phospho-Rb (1:500, Cell Signaling Technology, catalog no. 9307), total Rb (1:500, Cell Signaling Technology, catalog no. 9309), HuR (1:1,000, Life Technology/Thermo Fisher Scientific, catalog no. 390600), YAP1 (1A12; 1:500, Cell Signaling Technology, catalog no. 12395), cyclin D1 (1:500, Santa Cruz Biotechnology, catalog no. 8396), p27 (1:1,000, Santa Cruz Biotechnology, catalog no. sc-1641), and α-tubulin (1:5,000, Invitrogen, catalog no. A11126).

For IHC analysis, phospho-Rb (Cell Signaling Technology, catalog no. 8516), total Rb (Cell Signaling Technology, catalog no. 9309), and Ki67 (Roche, catalog no. 790-4286), and TUNEL (Trevigen TACS 2 TdT Core Kit, catalog no. 4810-30-CK) staining antibodies were used. For TUNEL staining, only diaminobenzidine (DAB) staining was used.

Genomic PCR. Total genomic DNA was extracted using the DNeasy Blood & Tissue Kits (Qiagen, catalog no. 69506) and 100 ng DNA was used per RT-PCR reaction using the Platinum Taq DNA Polymerase kit (Thermo Fisher Scientific, catalog no. 10966026). Samples were run on 0.75% agarose gel and LB buffer and imaged with UV box and camera. PCR SYBR primers were created by IDT and shown in Supplementary Figs. S1F and S3D. DNA sequencing was performed by Genewiz using Sanger sequencing methodology.

Quantitative real-time RT-PCR. Total RNA was extracted using the RNeasy Mini Kit (Qiagen, catalog no. 74106) and cDNA was made using 1,500 μg total RNA using Applied Biosystems High Capacity cDNA Reverse Transcriptase kit (Thermo Fisher Scientific, catalog no. 4368814) and quantitative PCR (qPCR) was performed using specific SYBR primers, as described above, and run on QuantStudio 3 (Thermo Fisher Scientific). Relative quantification was performed using the $2^{-\Delta\Delta C}{}_t$ method and comparing to GAPDH or 18s.

Transfection assays and HuR CRISPR assays. For transfections, Mia PaCa2 cells were seeded at 5×10^5 cells per 10-cm dish. The next day, transfection reagent (si negative control, siHuR or siYAP1) and Lipofectamine 2000 were added and transfected as described previously (29). Media were changed on cells the next day and 24 hours later the cells were split for either cell viability (Pico Green) experiments or Western blot experiments. Mia PaCa2 HuR CRISPR knockout cells were generated as described previously (28) and validated prior to use.

In vivo

Xenograft model information and dosing. Athymic female nude mice were purchased from Envigo at 6 weeks old and 20–25 g in size. Tumor growth was initiated by subcutaneous injection of 2×10^6 Mia PaCa2 cells in a 1:1 mixture of Matrigel and PBS on bilateral rear flanks of each subject animal. When mean tumor volumes reached approximately 100 mm^3 in size, the animals were randomized by tumor size into three groups with 5 mice/group. For efficacy studies, abemaciclib was dosed orally at 75 mg/kg, 0.1 mL/dose, daily Monday–Friday and the vehicle-only control group was given oral 1% hydroxyethyl cellulose (HEC) vehicle according to the same schedules. Mice body weight and tumor volumes were recorded three times per week, and once tumors reached a volume of 1,500 mm^3, the mice were euthanized. All animal studies were approved and performed in accordance with the Institutional Animal Care and Use Committee (IACUC) guidelines. Abemaciclib (MedChem Express, catalog no. HY-16297, lot no. 27360) was formulated daily in 1% HEC in 25 mmol/L phosphate buffer (PB; pH = 2).

Statistical analysis

Statistical analysis was performed using Prism (version 7.03) software. An independent two-tailed *t* test was utilized for comparison of mean percent change in tumor volume between placebo and treatment groups. A $P < 0.05$ is considered statistically significant. For the *in vivo* experiment, Grubb test was employed on all group values to assess for outliers and if any value was found to be positive for an outlier, it was excluded from statistical analysis. Grubb testing is available online along within GraphPad.

Results

Abemaciclib is effective against PDAC cells

Abemaciclib has been demonstrated to be a more potent inhibitor of CDK4/6 compared with the CDK4/6 inhibitors palbociclib and ribociclib *in vitro* (20). Therefore, we sought to define the efficacy of this drug in several PDAC cell lines; Mia PaCa2, Panc-1 (30), and HS 766T cells (31), three PDAC cell lines with characteristic loss of *CDKN2A* (Supplementary Fig. S1A). Palbociclib was published to be effective in PDAC in the past (2); therefore, we compared abemaciclib to palbociclib as an established benchmark. We found that across these three PDAC cell lines, abemaciclib had IC_{50} <1 μmol/L, and was comparable with palbociclib in all three cell lines (Fig. 1A). In long-term drug sensitivity assays, abemaciclib inhibited colony formation with IC_{50}s in the nanomolar range and was comparable with palbociclib at similar drug concentrations, as seen in Fig. 1B and Supplementary Fig. S1E. We also tested standard PDAC chemotherapeutics gemcitabine and oxaliplatin on PDAC cell lines and found abemaciclib was less effective at inhibiting cell survival as compared with gemcitabine, but more potent than oxaliplatin (Fig. 1C, HPNE comparison shown in Supplementary Fig. S1D).

To investigate the time dependency of abemaciclib effect on cell viability inhibition, we compared abemaciclib to no treatment over the course of 5 days. We found a statistically significant decrease in cellular viability of the abemaciclib-treated PDAC cell lines when compared with no treatment over days 3, 4, and 5 (Fig. 1D). This difference was most pronounced on day 5 in all three cell lines with a $P < 0.0001$. To validate these effects in more clinically relevant models, we determined the *CDKN2A* status of patient-derived xenografts (PDX, Supplementary Fig. S1A). The PDX lines were found to have a deletion of *CDKN2A* and

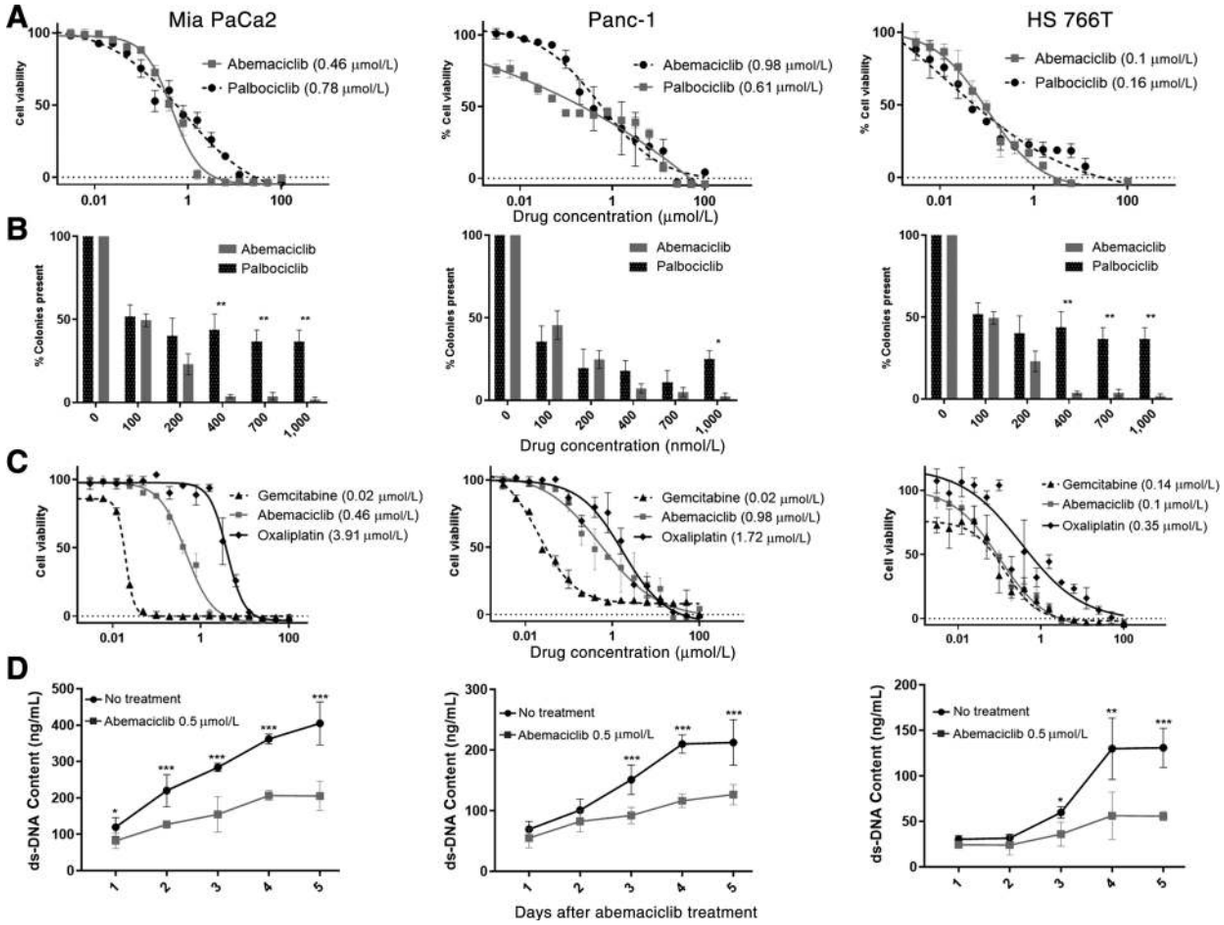

Figure 1.

Abemaciclib is effective *in vitro* in pancreatic cancer cell lines. **A,** Pico green assays to assess short-term drug response comparing abemaciclib to palbociclib in PDAC cells. IC_{50} values for both cell lines are shown in the parenthesis. **B,** Crystal violet staining to assess long-term drug responses comparing abemaciclib to palbociclib in PDAC cell. **C,** Pico green assays to compare PDAC standard-of-care chemotherapeutics gemcitabine and oxaliplatin to abemaciclib in PDAC cell lines. IC_{50} for both cell lines are shown in the parenthesis. **D,** Pico green assays comparing no treatment to abemaciclib-treated ds-DNA counts collected daily.

abemaciclib also had similar effects on cell viability (Supplementary Fig. S1B). To confirm the pathway, we compared the efficacy of abemaciclib in our KPC/KTC mouse organoid lines, which are wild-type *CDKN2A*, to *CDKN2A*-null mouse organoids generated from PKP mice (ref. 26; Supplementary Fig. S1A). We found that abemaciclib had slightly lower IC_{50} values in the *CDKN2A*-null organoids compared with *CDKN2A*-proficient KPC organoids (Supplementary Fig. S1C). In addition, abemaciclib had a significantly lower IC_{50} in Mia PaCa2, which is *CDKN2A* deficient, compared with normal pancreatic cell line HPNE, which is has *CDKN2A* preserved (Supplementary Fig. S1D).

Abemaciclib induces apoptosis

Abemaciclib's main mechanism of action has been demonstrated to be the inhibition of cell-cycle progression leading to senescence in Rb-positive cells (14, 21). In addition, abemaciclib has been reported in other cancer types to cause apoptosis (14, 23, 24). We sought to assess whether abemaciclib causes cell death, senescence, or both in our PDAC cells (Fig. 2A). We first assessed for cleaved caspase 3—an early marker of apoptosis upon abemaciclib treatment. We detected an increase in cleaved caspase 3 levels in Mia PaCa2 cells treated with abemaciclib compared with no treatment on days 1–3 of treatment, compared with staurosporine-treated cells that served as our positive control (Fig. 2B). To confirm these findings, we performed live-cell staining for caspase 3/7 activity and detected a significant increase in fluorescent caspase 3/7 cleavage activity (Fig. 2C) over days 1 and 2 in Mia PaCa2 cells ($P < 0.001$, $P < 0.025$, respectively). Similar results were obtained in Panc-1 and HS 766T cells (Fig. 2C). As a validating marker for early and late apoptosis, Annexin V staining was performed after 3 days of abemaciclib treatment. We detected an increase in apoptotic and dead cells when compared with no treatment in all cell lines. Upon further analysis, we found that there were more PDAC cells in early apoptosis (only Annexin V positive) compared with late apoptosis (both Annexin V and PI positive). Of note, Panc-1 had more cells in late apoptosis (both Annexin V and PI positive) after treatment (Fig. 2D; Supplementary Fig. S2A). Having demonstrated that there was significant induction of apoptosis at the time of treatment, we

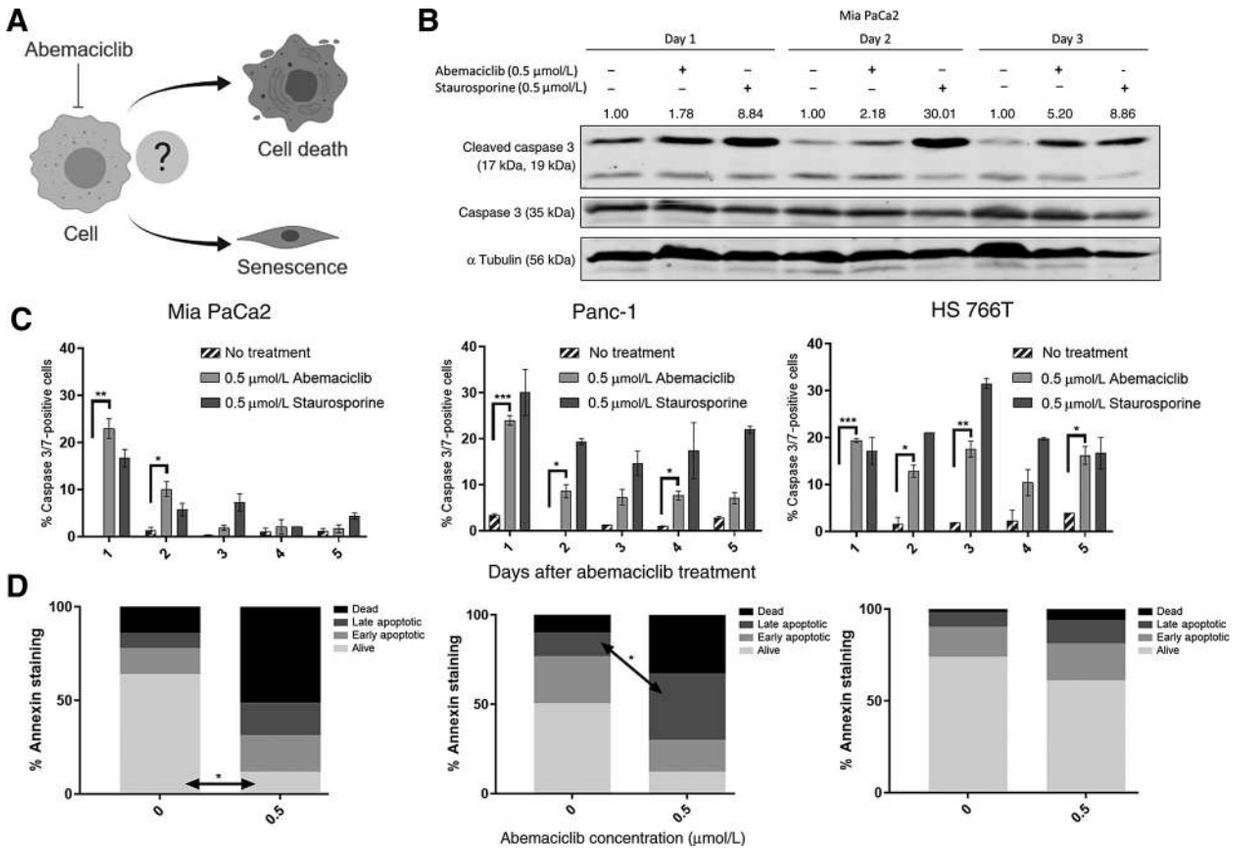

Figure 2.

Abemaciclib can kill PDAC cells and induce apoptosis. **A,** Schematic representation of possible fate of cells treated with abemaciclib either inducing apoptosis or senescence. **B,** Mia PaCa2 cells were treated with abemaciclib, or staurosporine as a positive control, and lysates were collected daily. Samples were run via Western blot analysis and probed for cleaved caspase 3 and total caspase 3. Quantification and normalization comparing cleaved caspase levels to total caspase levels. **C,** Quantification of activated caspase 3/7 counts over day 1–5 with treatment with abemaciclib, or staurosporine, in PDAC cell lines. **D,** Quantification of Annexin V flow cytometry analysis in PDAC cells with subgroup quantification of early and late apoptosis on the left bar graphs and total apoptosis on the right bar graphs, collected on day 3.

next sought to determine whether there was a concurrent arrest in cell-cycle progression in remaining live cells.

Abemaciclib causes G_1 arrest and inhibits cell-cycle progression

Abemaciclib's effect on cell-cycle progression was analyzed using phospho-Rb (pRb) immunoblot and BrdU incorporation analyses. BrdU is a florescent-labeled analogue of the DNA precursor thymidine and incorporates within dividing cells and can be used to track cells in G_1, S, and G_2 phases. Our results demonstrate that 3-day treatments with abemaciclib significantly reduced pRb expression in all three cell lines compared with no treatment (Fig. 3A). Abemaciclib treatment caused a dose-dependent inhibition of BrdU incorporation in Mia PaCa2, Panc-1, and HS 766T cell lines (Fig. 3B). In all three cell lines, there was approximately 50% decrease in BrdU incorporation starting at 0.010 μmol/L abemaciclib treatment (Fig. 3B) and at 0.5 μmol/L of abemaciclib over 75% of cells had a decrease in BrdU incorporation. Specifically, abemaciclib arrested cells in G_1–S phase (Fig. 3C) consistent with the downstream effects of Rb inactivation by CDK4/6 inhibitors (14, 32).

Abemaciclib induces senescence in PDAC cell lines

To determine whether abemaciclib induced senescence in PDAC cells, we first analyzed for β-galactosidase staining over a 7-day time period. Hydrogen peroxide (H_2O_2) served as an established positive control of early stress-induced senescence (refs. 33, 34; Supplementary Fig. S3A). To further validate our β-gal assay techniques, we tested previously published chemotherapeutics that have been demonstrated to induce a senescent phenotype [gemcitabine (35), irinotecan (36), 5-florouracil (37), oxaliplatin (38)], compared with paclitaxel that was not shown to induce senescence (Supplementary Fig. S3C). We found positive staining in cells as early as 2 days posttreatment with abemaciclib (Fig. 4A), consistent with senescence (14). In Mia PaCa2 and HS 766T cells, there was a peak at days 2–3 and then a plateau in β-gal–positive cells (Fig. 4C). Panc-1 cells, however, displayed a peak after 3 days of treatment. On days 5–7, approximately 75% of Mia PaCa2, 60% of HS 766T, and 40% of Panc-1 cells demonstrated strong β-gal staining indicating senescence (Fig. 4A–C). These cells also demonstrated classic senescent morphologic changes, appearing flat with spindle-shaped borders (ref. 39; Fig. 4B).

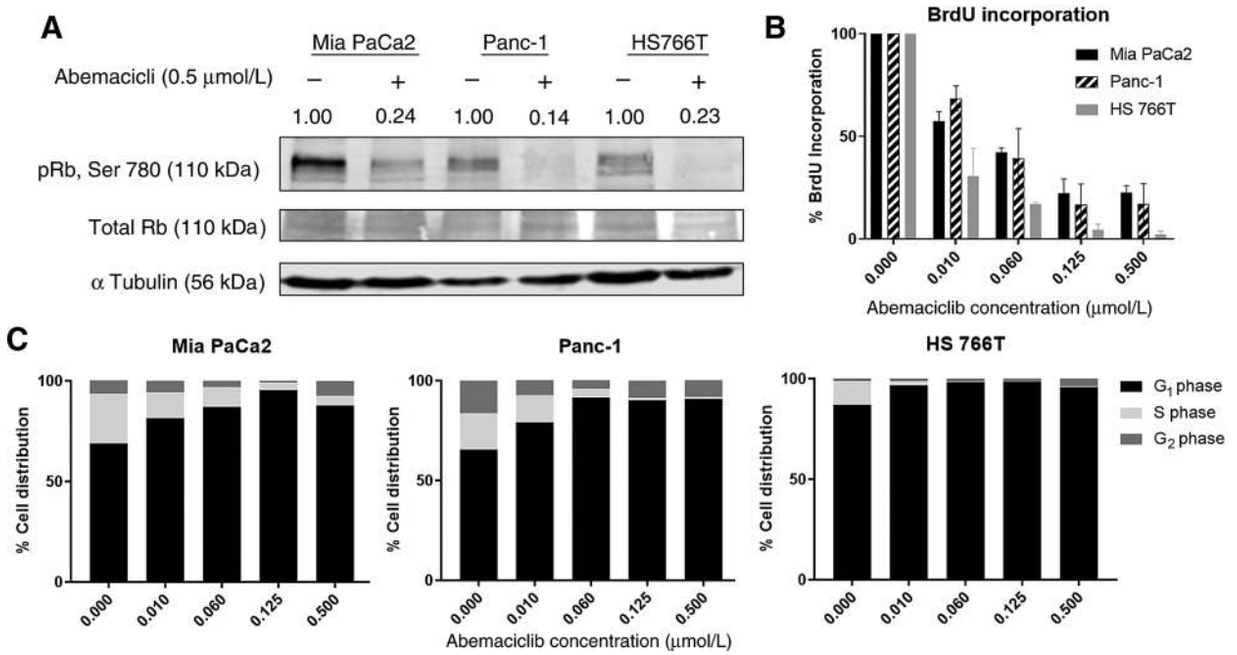

Figure 3.

Abemaciclib causes G_1 arrest and inhibits cell-cycle progression in PDAC cell lines. **A,** Western blot of PDAC cell lines treated with abemaciclib and probed for pRb. **B,** PDAC cell lines were treated with abemaciclib at indicated concentrations for 3 days and tested for BrdU incorporation via flow cytometry. Abemaciclib-treated cells were normalized to no treatment cells. **C,** Subgroup analysis of BrdU-incorporated cells in each phase of cell cycle: G_1, S, and G_2 phase, and graphed in bar plots per cell line and abemaciclib concentration.

Another well-characterized marker of senescence is increased levels of senescence-associated secretion (SASP) markers. To assess changes in these markers, mRNA was extracted from cells treated with abemaciclib or H_2O_2 and analyzed for SASP markers: IL1a, MCP 1/CCL2, and DCR2 (35) over the same 7-day period. Abemaciclib treatment significantly increased mRNA expression of multiple SASP markers in all three cell lines (Fig. 4D). In the Mia PaCa2 cells, abemaciclib significantly increased MCP2/CCL2 mRNA expression as early as day 1. In Panc-1 cells, there was a significant increase in MCP2/CCL2 and DCR2 mRNA markers and in HS 766T only DCR2 mRNA marker was significantly elevated after abemaciclib treatment. This trend correlated with β-gal staining (Fig. 4C and D) and shows 60%–75% of PDAC cells undergoing senescence after abemaciclib treatment. Finally, we sought to understand whether abemaciclib's senescence induction was due to reactive oxygen species (ROS) generation, as is the case with H_2O_2 ROS induction of stress-induced senescence (33). We performed a DCFDA cellular ROS labeling and detection assay on PDAC cells treated with H_2O_2 or abemaciclib over 7 days. We found that H_2O_2 increased DCFDA florescence (positive control) 24 hours after treatment, but abemaciclib did not cause any significant increase in DCFDA florescence even at day 7 (Supplementary Fig. S3B).

Abemaciclib inhibits pancreatic Mia PaCa2 xenograft tumor growth

In an *in vivo* study using Mia PaCa2 cells in a subcutaneous xenograft mouse model, we observed a significant decrease in tumor growth in the abemaciclib-treated arm versus control ($P < 0.0001$, Fig. 5A; Supplementary Fig. S4A) and the therapy was safe as demonstrated by mouse weights remaining within 10% of baseline (Fig. 5A). At the end of study, tumors were harvested and weighed (Fig. 5B), showing significant difference in tumor weights of abemaciclib-treated group compared with vehicle control.

Abemaciclib decreases pRb and Ki67 in vivo

Harvested tumors from the xenograft study were sectioned and stained for pRb, Rb, and Ki67. The abemaciclib-treated tumors demonstrated a decrease in pRb and total Rb expression compared with vehicle (Fig. 5C; Supplementary Fig. S4C). Pathologist scoring and quantification of IHC staining shows that in the abemaciclib-treated tumors, there were 46.3% cells with positive pRb staining, compared with no treatment that had 74.5% cells with positive pRb. In addition, compared with no treatment that had 78.8% cells with positive Ki67 staining, the abemaciclib-treated tumors had 59.5% cells with positive Ki67 staining (Fig. 5D). Overall, when normalized to no treatment, abemaciclib-treated tumors had approximately 38% reduction in pRb staining, and 25% reduction in pRb/total Rb staining along with Ki67 staining (Fig. 5D). Compared with vehicle alone, abemaciclib-treated tumors had weak TUNEL-positive staining (Fig. 5D). RNA extracted from these tumors were probed for SASP markers indicative of senescence and we found significant increases in IL1a, MCP1/CCL2, and DCR2 mRNA, in the abemaciclib-treated tumors when compared with vehicle alone (Fig. 5E). These results demonstrate that abemaciclib treatment induces apoptosis, decreases pRb and tumor growth, and induces senescence in this *in vivo* xenograft model.

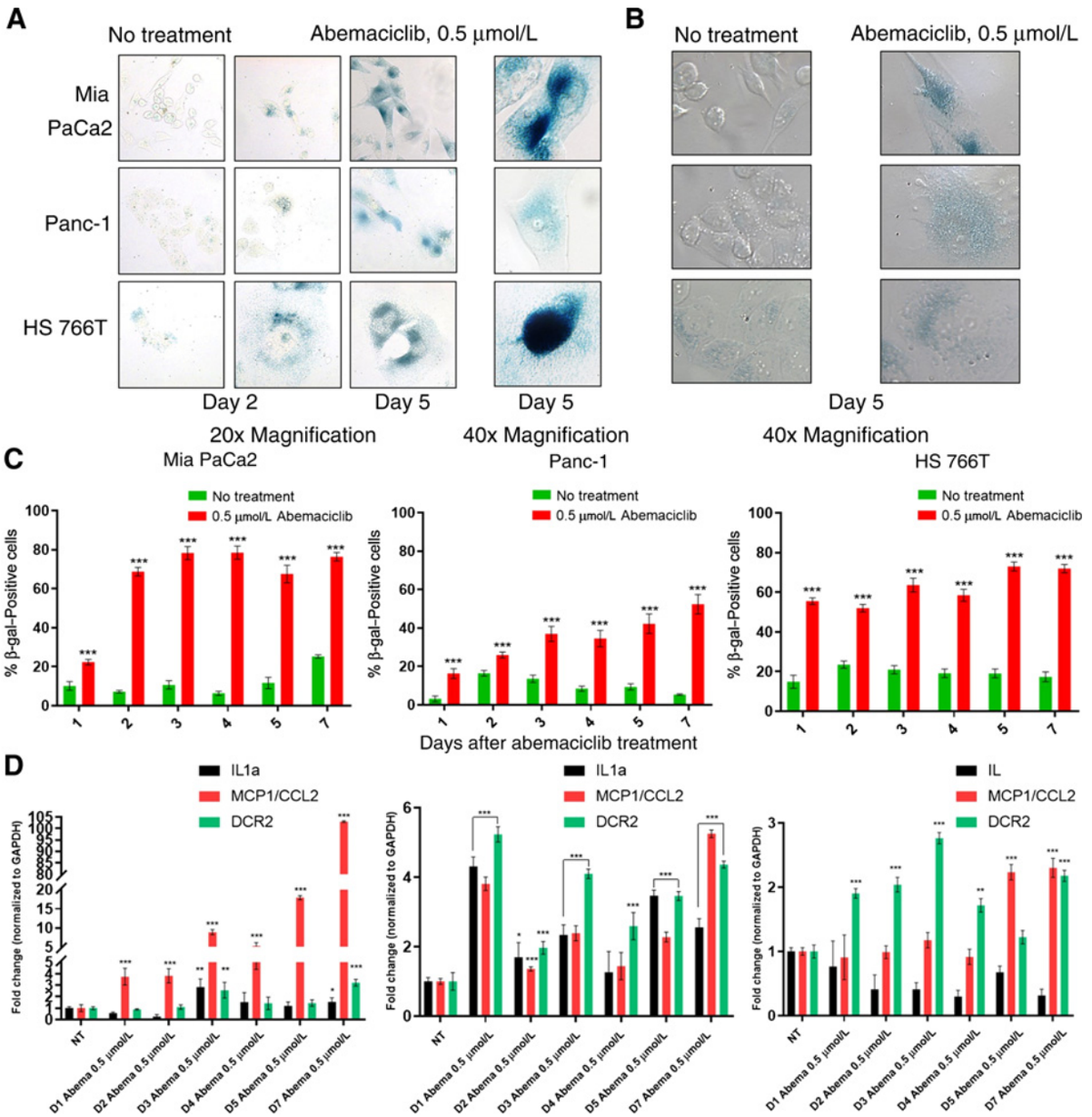

Figure 4.

Abemaciclib induces senescence in pancreatic cancer cell lines. **A,** Representative β-gal images of PDAC cell lines either treated with abemaciclib or no treatment and collected at days 2 and 5. Positive β-gal imaging is indicated by blue color in senescent cells, shown with 20× and 40× magnification. **B,** Morphologic changes as seen in no treatment compared with abemaciclib-treated cells in PDAC cell lines, seen on 40× magnification. **C,** Quantification of total β-gal–positive counts over total cells present for abemaciclib-treated cell and no treatment cells collected daily for 7 days. **D,** qPCR results of cells treated with abemaciclib or H_2O_2, compared with no treatment, evaluating for SASP markers. Samples were collected daily and normalized to the same day no treatment. Significance is denoted as *, $P < 0.05$; **, $P < 0.005$; ***, $P < 0.0005$.

A pilot synergy drug screen identifies novel targeting strategies to enhance abemaciclib therapy

To determine whether any of the drugs standardly used in PDAC synergized with abemaciclib, we evaluated synergism of abemaciclib with standardly used PDAC therapeutics using the Loewe synergism method (40). Our initial panel covered the components of FOLFIRINOX (Supplementary Fig. S5A), as well as gemcitabine and paclitaxel (Fig. 6A; Supplementary Fig. S5B); unfortunately, we did not find any significant synergism with these standard-of-care agents except for weak synergy with 5-FU. As we did not observe significant synergy with standard therapeutics, we wanted to determine whether other targeted therapeutics may synergize more potently with abemaciclib in PDAC.

Our lab has extensively characterized the importance of the mRNA-binding protein, Human Antigen R (HuR), as an essential mediator of PDAC cell survival and chemotherapeutic

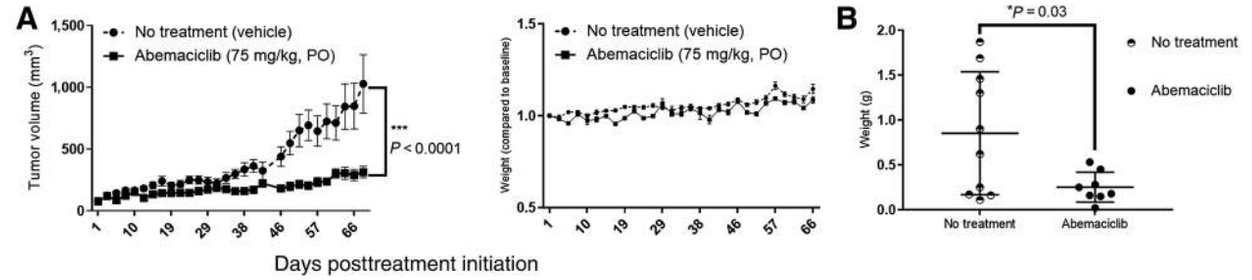

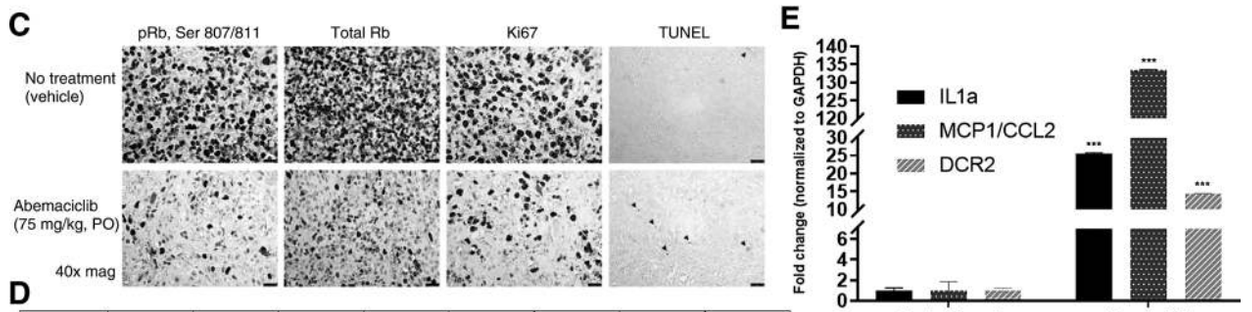

D

	pRb % positive	Normalized pRb ratio (%)	Total Rb % positive	pRb/ total Rb ratio	Normalized pRb/Rb ratio (%)	Ki67 % positive	Normalized Ki67 ratio (%)	Raw TUNNEL count
No treatment	74.5	100	83.9	0.89	100	78.8	100	1
Abemaciclib	46.3	62.1	68.2	0.68	76.4	59.5	75.5	5

Figure 5.

Abemaciclib is able inhibit pancreatic Mia PaCa2 xenograft tumor growth *in vivo.* **A,** Mia PaCa2 cells were injected in a xenograft flank model. Tumor volume measurements were calculated and plotted over time for the no treatment vehicle only arm ($n = 5$) or abemaciclib, 75 mg/kg orally, daily ($n = 4$). Mouse weights were also recorded and plotted over time. Note: 1 mouse in the abemaciclib treatment arm was removed from analysis, as it was an outlier per Grubb outlier testing using Prism software (Supplementary Fig. S5B). **B,** Tumors collected at the end of the experiment were weighed on day of harvest and plotted for each arm. **C,** IHC analysis of paraffin-embedded xenograft tumors and probed for pRb, ser 807/811, total Rb, Ki67 looking at proliferative index, and TUNEL looking at DNA fragmentation. On TUNEL staining, black arrows pointing toward positively stained nuclei. **D,** Pathologist-scored quantification of nuclear pRb, total Rb, and Ki67 staining was performed and tabulated. Ratios were generated to the amount of pRb to total Rb, or Ki67, and normalized to no treatment. TUNNEL-positive cells were counted by hand. **E,** qPCR results of tumor samples collected at the end of the experiment. mRNA was extracted from tumors and evaluated for SASP markers. Samples were normalized to no treatment (vehicle); significance is denoted as *, $P < 0.05$; **, $P < 0.005$; ***, $P < 0.0005$.

resistance (28, 41). Importantly, HuR is a critical regulator of cyclin D1, with loss of HuR leading to a dramatic decrease in cyclin D1 expression at the mRNA and protein level (42, 43). Therefore, we hypothesized that CDK4/6 inhibition combined with HuR inhibition could provide an enhanced response and increased sensitivity to abemaciclib. We found synergism with two published HuR inhibitors, pyrvinium pamoate (44) and CMLD2 (41) when dosed in combination with abemaciclib in Mia PaCa2 cells (Fig. 6A; Supplementary Fig. S5B) or with Panc-1 cells (Fig. 6B; Supplementary Fig. S5B) in a short-term Pico green assay.

Yes-Associated Protein 1 (YAP1) is a transcriptional coactivator that is a critical regulator of PDAC development (45) and is also a known regulator of cyclin D1 (46) and CDK6 (47, 48). It has also previously been demonstrated that inhibition synergizes with CDK4/6 inhibitors in esophageal cancer (48) and thus, we tested the ability of YAP-1 inhibitors to synergize with abemaciclib treatment in PDAC. We observed synergism in PDAC cells treated with abemaciclib and the YAP-1 inhibitors verteporfin (49) and CA3 (ref. 48; Fig. 6A and B; Supplementary Fig. S5B).

To assess for synergistic combinations in a long-term assay, we performed colony-forming assays with abemaciclib and the HuR and YAP1 inhibitors that were found to be synergistic in long-term drug sensitivity assay as well (Fig. 6C and D). We found that in both Mia PaCa2 and Panc-1, the combination of abemaciclib with either a HuR inhibitor or YAP1 inhibitor was able to decrease the number of colonies than monotherapy (Fig. 6C and D).

To validate the role of HuR loss and abemaciclib, we tested abemaciclib in our Mia PaCa2 HuR CRISPR KO cells (ref. 28; CRISPR KO validation data; Supplementary Fig. S6C) and found that there was a decrease in abemaciclib's IC_{50} in two different CRISPR KO clones (*ELAVL1*$^{-/-}$) when compared with the parental cell lines (Supplementary Fig. S6A) confirming our HuR inhibitor data. In these HuR KO cells, there was a more significant decrease in pRb levels after abemaciclib treatment compared with parental cells (*ELAVL1*$^{+/+}$) that were treated with abemaciclib (Supplementary Fig. S6B).

As a secondary method to confirm that inhibition of HuR or YAP1 increased abemaciclib's sensitivity in PDAC cells, we transfected cells with either siHuR or siYAP1 oligonucleotides. When compared with si negative control, cells transfected with siHuR and siYAP1 had a lower IC_{50}s for abemaciclib treatment compared with si negative control cells, demonstrating an increase in sensitivity for abemaciclib due to HuR or YAP1 silencing (Supplementary Fig. S6D). We validated target knockdown by Western blot analysis and found there was a 67% knockdown of HuR and 90% knockdown of YAP1, as compared with control cells, three days after transfection had taken place (Supplementary Fig. S6E).

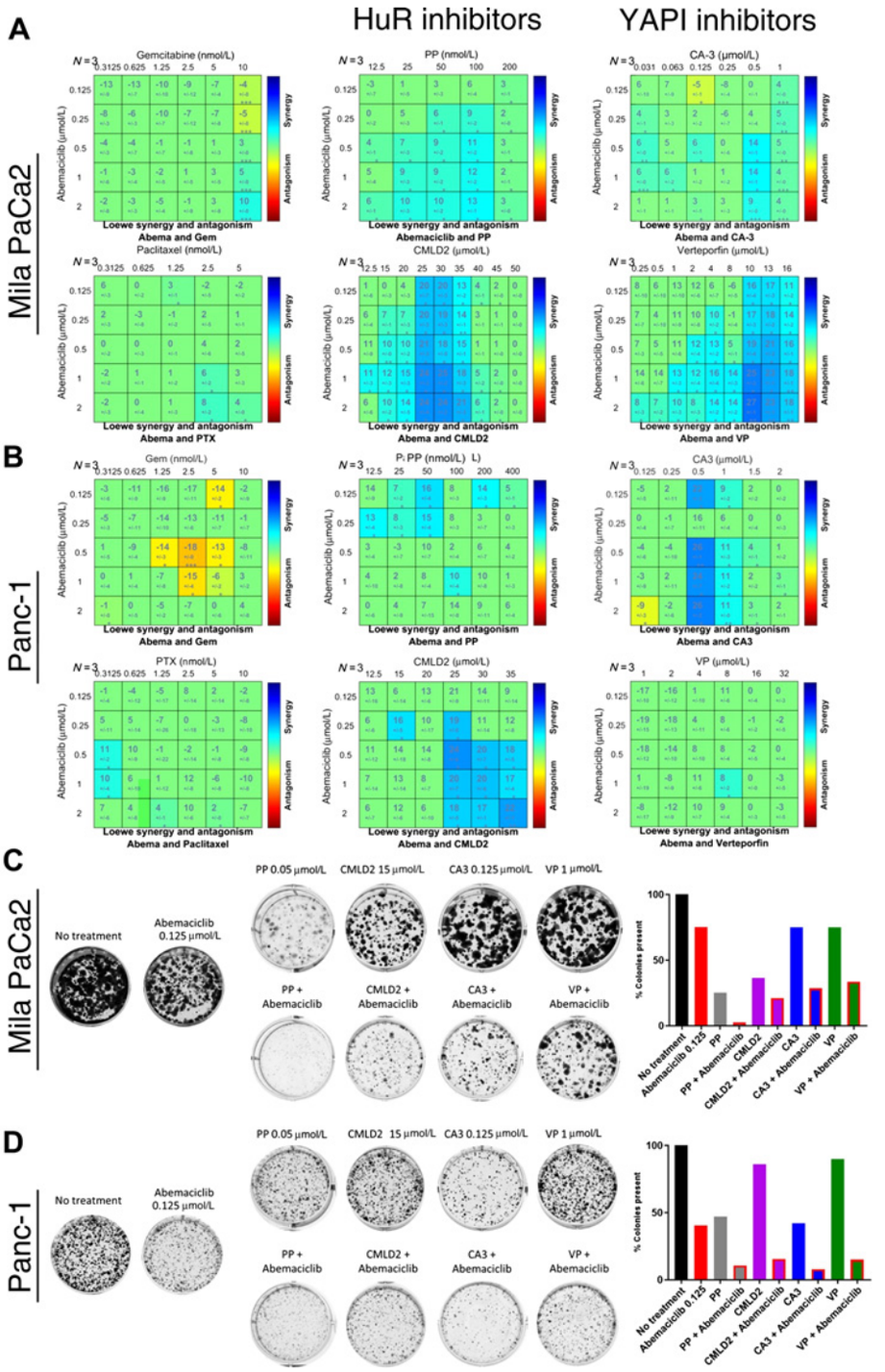

Figure 6.

Abemaciclib is synergistic with HuR and YAP1 inhibitors. **A,** Loewe synergy plots for Mia PaCa2 cells treated with abemaciclib and the listed compounds. Supplementary Figure S6B shows percent viability corresponding to the synergistic combinations shown. **B,** Loewe synergy plots for Panc-1 cells treated with abemaciclib and the listed compounds. Supplementary Figure S6B shows percent viability corresponding to the synergistic combinations shown. **C,** Long-term colony formation assay in Mia PaCa2 cells collected after 10 days of drug treatment, as single agent, or in combination. Images on the left are from the colonies seen, and quantification of the colonies are shown on the right. All quantifications were done using ImageJ. Combination concentrations were taken from synergy plots shown in **A** and **B**. **D,** Long-term colony-formation assay in Panc-1 cells collected after 10 days of drug treatment, as a single agent or in combination. Images on the left are from the colonies seen, and quantification of the colonies are shown on the right. All quantifications were done using ImageJ. Combination concentrations were taken from synergy plots shown in **A** and **B**.

Inhibition of HuR and YAP1 is synergistic with abemaciclib, likely through the cyclin D1 pathway

Abemaciclib treatment lead to a decrease in pRb in all the samples compared with their no treatment counterparts, and in the siRNA negative control sample, led to an increase in cyclin D1 (Supplementary Fig. S6E). Increased expression of cyclin D1 after CDK4/6 inhibition has been seen in other models (19) and has been linked to a possible mode of CDK4/6 resistance, but interestingly, after HuR or YAP1 knockdown, there is no increase in cyclin D1 protein levels in the abemaciclib-treated samples (Supplementary Fig. S6E). To confirm that cyclin D1 is regulated by HuR in our cell culture model, we performed an HuR RNA immunoprecipitation assay (RIP) and probed for p27, cyclin D1, and an established HuR target PIM1 (ref. 28; Supplementary

Fig. S6F). Compared with IgG, we found significant increases in cyclin D1, p27, and our positive control PIM1 ($P < 0.0001$) in the HuR pulldown mRNA (Supplementary Fig. S6F).

To assess whether synergism between abemaciclib and HuR or YAP1 inhibition was through their shared regulation of cyclin D1 (42, 43, 46), we transfected cells with si cyclin D1 oligonucleotides. Because of the finding that cells transfected with si cyclin D1 grew slower than the negative control cells, we calculated GR_{50}s to compare between the two conditions. When compared with si negative control, cells transfected with si cyclin D1 had a lower IC_{50} for abemaciclib treatment compared with siControl cells, demonstrating an increase in sensitivity for abemaciclib due to cyclin D1 silencing (Supplementary Fig. S6G). We validated target knockdown by Western blot analysis (Supplementary Fig. S6H) and found there was a 63% knockdown of cyclin D1 three days after the transfection had taken place (Supplementary Fig. S6H). In addition, in the si cyclin D1 abemaciclib-treated samples, there was no further increase in cyclin D1 levels when compared with the abemaciclib-treated si negative control sample (Supplementary Fig. S6H), validating what we had seen earlier with the siHuR and siYAP1 abemaciclib-treated cells (Supplementary Fig. S6E).

Chronic treatment with abemaciclib leads to decreased sensitivity to gemcitabine, but not to HuR or YAP1 inhibitors

To model the potential effects and resistance mechanisms caused by long-term abemaciclib therapy in patients, Mia PaCa2 and Panc-1 cells were cultured with increasing concentrations of abemaciclib for 10–12 months to create abemaciclib-resistant clones. These cells had a 2- to 4-fold increase in GR_{50} in the "chronic" abemaciclib therapy cells (meaning these cells were less sensitive) when treated with abemaciclib indicating a resistance phenotype (Fig. 7A–C). To evaluate whether these "chronic" abemaciclib therapy cells had any increased or decreased responsiveness to other chemotherapeutics, we calculated GR_{50} on common components of FOLFIRINOX, along with HuR and YAP1 inhibitors used earlier. As seen in Fig. 7B and C, we found that both the Mia PaCa2 and Panc-1 "chronic" abemaciclib therapy cells were more resistant to gemcitabine and 5-FU but remained sensitive to pyrvinium pamoate (HuR inhibitor) and verteporfin (YAP1 inhibitor). In addition, when these "chronic" abemaciclib therapy cells were treated with abemaciclib and gemcitabine in combination, we found antagonistic drug combinations, but when we treated these "chronic" abemaciclib therapy cells with HuR inhibitor, CMLD2, or YAP1 inhibitors, CA3 or verteporfin, in combination and abemaciclib, there was increase of abemaciclib with HuR and YAP-1 inhibitors (Fig. 7D and E). These findings demonstrate that the Mia PaCa2 "chronic" abemaciclib therapy cells have more significant synergy with these compounds compared with that of the parental cell line in Fig. 6A and B. Finally, to understand whether these "chronic" abemaciclib therapy cells were able to maintain their resistance to abemaciclib after removal of drug therapy, we removed abemaciclib for 21 days and compared GR_{50}s in these cell lines. In both Mia PaCa2 and Panc-1 "chronic" abemaciclib therapy lines, we found that once we removed abemaciclib from the media these cells had phenotypes similar to their parental counterpart cells. We observed that as early as 14 days and 21 days without abemaciclib, these "chronic" abemaciclib (CA)-treated cells had decrease in GR50 to abemaciclib, as seen in Supplementary Fig. S7A. Although these "chronic" abemaciclib–treated cells stained positive for β-gal (Supplementary Fig. S7B), they did not have elevations in SASP markers (Supplementary Fig. S7C), indicating that the positive staining is likely due to stress-induced senescence.

Discussion

The premise for studying CDK4/6 inhibition in PDAC cells has been well established (2, 7, 18, 19). Specifically, the CDK4/6 inhibitor, abemaciclib's effects in breast cancer and other solid tumor types have been well characterized (14, 20–22, 50), but little is known about its effect in PDAC. We demonstrate that abemaciclib treatment caused inhibition of pRb and induced senescence *in vitro* and a decrease in tumor volume *in vivo*. In addition, we found a reduction in total Rb *in vivo*, as was seen in other tumor models including breast cancer and melanoma (50).

As most recent positive clinical trials for patients with pancreatic cancer have involved combination therapies (5, 51), we performed a focused drug screen to identify agents that would synergize with abemaciclib in PDAC cells. Previously, it has been reported that palbociclib is synergistic with gemcitabine in PDAC (18) and abemaciclib is synergetic with gemcitabine in lung cancer (52). Our data demonstrate an additive nature between abemaciclib and gemcitabine in PDAC (Fig. 6A and B). In addition, synergism was observed between abemaciclib and HuR and YAP1 inhibitors. We confirmed targeting of these small molecules with siRNA silencing of HuR and YAP1 in PDAC cells. Mechanistically, rationale exists to explain the synergy of combining abemaciclib with inhibition of HuR and YAP1, as both HuR and YAP1 can regulate cyclin D1 (42, 43, 46). Muralidharan and colleagues (42) found that treatment with siHuR oligos in a lung cancer model lead to downregulation of cyclin D1 and upregulation of p27, both of which are important for cell-cycle regulation and interaction with the cyclin D1–CDK4/6 complex (42). In addition, Li and colleagues (48) has published that YAP1 inhibition, using the inhibitor CA3, was synergistic with CDK6 inhibition in esophageal cancer both *in vitro* and *in vivo* (48). The combined effects of abemaciclib and HuR inhibition or YAP1 inhibition on the same cyclin D1/ CDK4/6 axis could logically explain the synergism we observed. Along with validating that cyclin D1 pulls down with HuR via RIP (Supplementary Fig. S6F), we have observed that by targeting cyclin D1, we were able to sensitize cells to abemaciclib treatment (Supplementary Fig. S6G).

In addition to studying synergistic drug combinations in PDAC cells, we sought to make abemaciclib-resistant cell lines to understand resistance mechanisms and to model the potential effects of long-term abemaciclib therapy on patients. Knudsen and colleagues recently published a review discussing mechanism of resistance to CDK4/6 inhibitors (19). They found that although the mechanisms for CDK4/6 inhibitor resistance are not fully elucidated, there are important drivers in the AKT, mTOR, and cyclin D1 pathways to promote resistance (19). In breast cancer models, upregulation of AKT is linked to the accumulation of cyclin D1, and in pancreatic cancer models upregulation of cyclin D1 can be decreased by using mTOR inhibitors (19). Cyclin D1 has an important role in developing acquired resistance to CDK4/6 inhibitors, although this mechanism is unclear (19). To assess an abemaciclib-resistant phenotype, we attempted to create abemaciclib-resistant cell lines. After 10–12 months of abemaciclib treatment, these "chronic" abemaciclib therapy cells had a

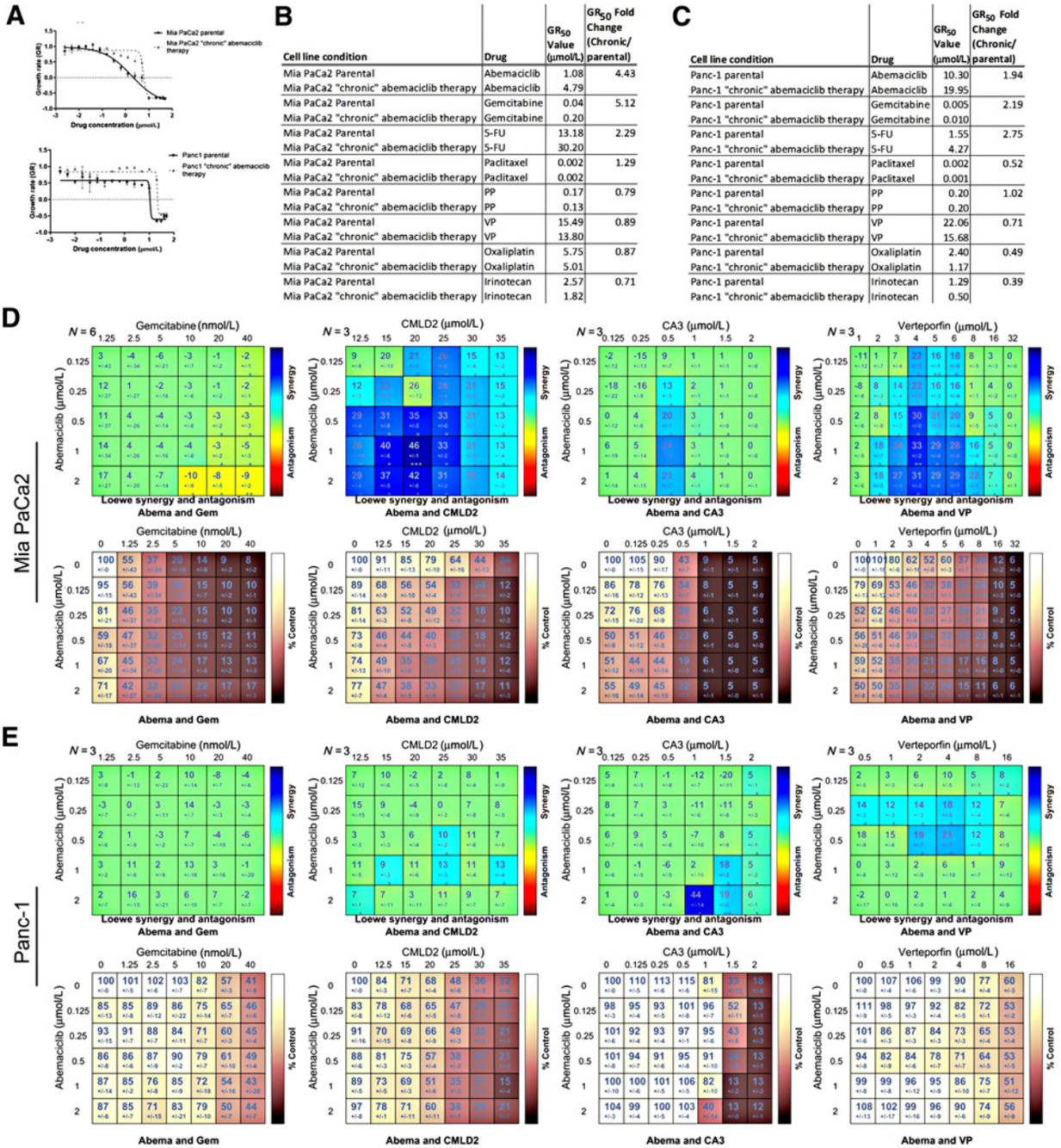

Cell line condition	Drug	GR_{50} Value (μmol/L)	GR_{50} Fold Change (Chronic/ parental)
Mia PaCa2 Parental	Abemaciclib	1.08	4.43
Mia PaCa2 "chronic" abemaciclib therapy	Abemaciclib	4.79	
Mia PaCa2 Parental	Gemcitabine	0.04	5.12
Mia PaCa2 "chronic" abemaciclib therapy	Gemcitabine	0.20	
Mia PaCa2 Parental	5-FU	13.18	2.29
Mia PaCa2 "chronic" abemaciclib therapy	5-FU	30.20	
Mia PaCa2 Parental	Paclitaxel	0.002	1.29
Mia PaCa2 "chronic" abemaciclib therapy	Paclitaxel	0.002	
Mia PaCa2 Parental	PP	0.17	0.79
Mia PaCa2 "chronic" abemaciclib therapy	PP	0.13	
Mia PaCa2 Parental	VP	15.49	0.89
Mia PaCa2 "chronic" abemaciclib therapy	VP	13.80	
Mia PaCa2 Parental	Oxaliplatin	5.75	0.87
Mia PaCa2 "chronic" abemaciclib therapy	Oxaliplatin	5.01	
Mia PaCa2 Parental	Irinotecan	2.57	0.71
Mia PaCa2 "chronic" abemaciclib therapy	Irinotecan	1.82	

Cell line condition	Drug	GR_{50} Value (μmol/L)	GR_{50} Fold Change (Chronic/ parental)
Panc-1 parental	Abemaciclib	10.30	1.94
Panc-1 "chronic" abemaciclib therapy	Abemaciclib	19.95	
Panc-1 parental	Gemcitabine	0.005	2.19
Panc-1 "chronic" abemaciclib therapy	Gemcitabine	0.010	
Panc-1 parental	5-FU	1.55	2.75
Panc-1 "chronic" abemaciclib therapy	5-FU	4.27	
Panc-1 parental	Paclitaxel	0.002	0.52
Panc-1 "chronic" abemaciclib therapy	Paclitaxel	0.001	
Panc-1 parental	PP	0.20	1.02
Panc-1 "chronic" abemaciclib therapy	PP	0.20	
Panc-1 parental	VP	22.06	0.71
Panc-1 "chronic" abemaciclib therapy	VP	15.68	
Panc-1 parental	Oxaliplatin	2.40	0.49
Panc-1 "chronic" abemaciclib therapy	Oxaliplatin	1.17	
Panc-1 parental	Irinotecan	1.29	0.39
Panc-1 "chronic" abemaciclib therapy	Irinotecan	0.50	

Figure 7:

Cells chronically treated with abemaciclib appear to be resistant to gemcitabine, but not to HuR or YAP1 inhibitors. **A,** Pico Green assay to calculate GR_{50} values for Mia PaCa2 parental cells and Mia PaCa2 "chronic" abemaciclib therapy cell lines treated with abemaciclib (top). Bottom, GR_{50} values comparing Panc-1 parental cells and Panc-1 "chronic" abemaciclib therapy cells treated with abemaciclib (bottom). **B,** Growth rate inhibition (GR_{50}) tables comparing Mia PaCa2 parental cells to Mia PaCa2 "chronic" abemaciclib therapy cells and treated with various chemotherapeutics including gemcitabine, pyrvinium pamoate (PP) and verteporfin (VP). Fold change was calculated comparing GR_{50} (μmol/L) value of "chronic" abemaciclib therapy cells to parental cells. **C,** Growth rate inhibition (GR_{50}) tables comparing Panc-1 parental cells to Panc-1 "chronic" abemaciclib therapy cells and treated with various chemotherapeutics including gemcitabine, pyrvinium pamoate and verteporfin. Fold change was calculated comparing GR_{50} (μmol/L) value of "chronic" abemaciclib therapy cells to parental cells. **D,** Loewe synergy plots for Mia PaCa2 "chronic" abemaciclib therapy cells treated with various compounds (top) with the corresponding percent viability (bottom). **E,** Loewe synergy plots for Panc-1 "chronic" abemaciclib therapy cells treated with various compounds (top) with the corresponding percent viability (bottom).

decrease in growth rate and were more resistant to both abemaciclib, gemcitabine, and 5-FU therapy, but not to HuR/ YAP1 inhibitors. This may be simply due to the cells not proliferating as rapidly, and therefore, these cells may be less sensitive to chemotherapeutics and antimetabolites that are ineffective in nondividing cells. Alternatively, these findings may offer further evidence that HuR/YAP1 inhibitors may work well with abemaciclib in treating patients with PDAC. Although the resistance to abemaciclib appeared to be a transient response, as these cells regained sensitivity to abemaciclib 2–3 weeks after the cells were removed from chronic abemaciclib exposure. Further investigation into the biology of these "chronic" abemaciclib therapy cells may give us new insights on possible drug combinations that can be used to break resistance in PDAC cells or provide information for next line treatment options (i.e., post-abemaciclib therapy).

Taken together, we present a promising preclinical evaluation of abemaciclib in both PDAC *in vitro* and *in vivo* models. Importantly, we were able to identify novel synergy between abemaciclib and HuR/ YAP1 inhibitors, as potential clinically relevant combination therapies to treat this deadly disease. Further investigations are warranted to properly characterize HuR/YAP1 inhibitors and these drug combination therapies, with the goal to test the best combination for the treatment of PDAC. Even though more diverse and sophisticated models could be used to evaluate abemaciclib-based therapies, we strongly believe these studies support the notion for a clinical trial evaluating abemaciclib in patients with PDAC.

Disclosure of Potential Conflicts of Interest

T. Golan reports receiving commercial research grants from MSD Merck and, AstraZeneca, has received speakers bureau honoraria from Abbvie, and has a consultant/advisory board relationship with Abbvie, AstraZeneca, and Teva. No potential conflicts of interest were disclosed by the other authors.

Authors' Contributions

Conception and design: T. Dhir, C.W. Schultz, S.Z. Brown, J. Posey, J.R. Brody
Development of methodology: T. Dhir, C.W. Schultz, A. Jain, S.Z. Brown
Acquisition of data (provided animals, acquired and managed patients, provided facilities, etc.): T. Dhir, C.W. Schultz, A. Haber, A. Goetz, C. Xi, W. Jiang, T. Golan
Analysis and interpretation of data (e.g., statistical analysis, biostatistics, computational analysis): T. Dhir, C.W. Schultz, A. Jain, A. Goetz, W. Jiang, C.J. Yeo, M.J. Pishvaian, J.R. Brody
Writing, review, and/or revision of the manuscript: T. Dhir, C.W. Schultz, A. Jain, S.Z. Brown, A. Haber, G.H. Su, W. Jiang, C.J. Yeo, T. Golan, M.J. Pishvaian, J.R. Brody
Administrative, technical, or material support (i.e., reporting or organizing data, constructing databases): T. Dhir, C.W. Schultz, L. Xu, C.J. Yeo
Study supervision: G.H. Su, J.R. Brody

Acknowledgments

This study was performed with grant support from the Newell Devalpine Foundation, 1R01CA212600-01 (to J.R. Brody) and T32 training grant NIH/ NIGMS T32GM008562 (to T. Dhir). This work was also supported, in part, by a National Cancer Institute of the National Institutes of Health under a Cancer Center Support Grant 5P30CA056036-17 (SKCC, TJU). This study was not funded by Eli Lilly and Company. IHC slides were processed and stained by Raymond O'Neill, Medical Technologist at Thomas Jefferson University Hospital (Philadelphia, PA).

The costs of publication of this article were defrayed in part by the payment of page charges. This article must therefore be hereby marked *advertisement* in accordance with 18 U.S.C. Section 1734 solely to indicate this fact.

Received June 4, 2019; revised July 29, 2019; accepted July 31, 2019; published first August 5, 2019.

References

1. Raman P, Maddipati R, Lim KH, Tozeren A. Pancreatic cancer survival analysis defines a signature that predicts outcome. PLoS One 2018;13: e0201751.
2. Franco J, Witkiewicz AK, Knudsen ES. CDK4/6 inhibitors have potent activity in combination with pathway selective therapeutic agents in models of pancreatic cancer. Oncotarget 2014;5:6512–25.
3. Tamburrino D, Partelli S, Crippa S, Manzoni A, Maurizi A, Falconi M, et al. Selection criteria in resectable pancreatic cancer: a biological and morphological approach. World J Gastroenterol 2014;20:11210–5.
4. Chapman BC, Gleisner A, Rigg D, Messersmith W, Paniccia A, Meguid C, et al. Perioperative and survival outcomes following neoadjuvant FOLFIRINOX versus gemcitabine abraxane in patients with pancreatic adenocarcinoma. JOP 2018;19:75–85.
5. Neoptolemos JP, Palmer DH, Ghaneh P, Psarelli EE, Valle JW, Halloran CM, et al. Comparison of adjuvant gemcitabine and capecitabine with gemcitabine monotherapy in patients with resected pancreatic cancer (ESPAC-4): a multicentre, open-label, randomised, phase 3 trial. Lancet 2017;389:1011–24.
6. Subramaniam D, Periyasamy G, Ponnurangam S, Chakrabarti D, Sugumar A, Padigaru M, et al. CDK-4 inhibitor P276 sensitizes pancreatic cancer cells to gemcitabine-induced apoptosis. Mol Cancer Ther, 2012;11:1598–608.
7. Heilmann AM, Perera RM, Ecker V, Nicolay BN, Bardeesy N, Benes CH, et al. CDK4/6 and IGF1 receptor inhibitors synergize to suppress the growth of p16INK4A-deficient pancreatic cancers. Cancer Res 2014;74: 3947–58.
8. Tang B, Li Y, Qi G, Yuan S, Wang Z, Yu S, et al. Clinicopathological significance of CDKN2A promoter hypermethylation frequency with pancreatic cancer. Sci Rep 2015;5:13563.
9. Calbo J, Serna C, Garriga J, Graña X, Mazo A. The fate of pancreatic tumor cell lines following p16 overexpression depends on the modulation of CDK2 activity. Cell Death Differ 2004;11:1055–65.
10. Sherr CJ, Roberts JM. CDK inhibitors: positive and negative regulators of G1-phase progression. Genes Dev 1999;13:1501–12.
11. Narasimha AM, Kaulich M, Shapiro GS, Choi YJ, Sicinski P, Dowdy SF, et al. Cyclin D activates the Rb tumor suppressor by mono-phosphorylation. Elife 2014;3.
12. Weinberg RA.The retinoblastoma protein and cell cycle control. Cell 1995;81:323–30.
13. Haberichter T, Mädge B, Christopher RA, Yoshioka N, Dhiman A, Miller R, et al. A systems biology dynamical model of mammalian G1 cell cycle progression. Mol Syst Biol 2007;3:84.
14. Torres-Guzman R, Calsina B, Hermoso A, Baquero C, Alvarez B, Amat J, et al. Preclinical characterization of abemaciclib in hormone receptor positive breast cancer. Oncotarget 2017;8:69493–507.
15. Al-Aynati MM, Radulovich N, Ho J, Tsao MS. Overexpression of G1-S cyclins and cyclin-dependent kinases during multistage human pancreatic duct cell carcinogenesis. Clin Cancer Res 2004;10:6598–605.
16. Cabrera MC, Díaz-Cruz ES, Kallakury BV, Pishvaian MJ, Grubbs CJ, Muccio DD, et al. The CDK4/6 inhibitor PD0332991 reverses epithelial dysplasia associated with abnormal activation of the cyclin-CDK-Rb pathway. Cancer Prev Res 2012;5:810–21.
17. Sathe A, Koshy N, Schmid SC, Thalgott M, Schwarzenböck SM, Krause BJ, et al. CDK4/6 Inhibition controls proliferation of bladder cancer and transcription of RB1. J Urol 2016;195:771–9.
18. Chou A, Froio D, Nagrial AM, Parkin A, Murphy KJ, Chin VT, et al. Tailored first-line and second-line CDK4-targeting treatment combinations in mouse models of pancreatic cancer. Gut 2017;67:2142–55.

19. Knudsen ES, Witkiewicz AK. The strange case of CDK4/6 inhibitors: mechanisms, resistance, and combination strategies. Trends Cancer 2017;3:39–55.
20. O'Leary B, Finn RS, Turner NC. Treating cancer with selective CDK4/6 inhibitors. Nat Rev Clin Oncol 2016;13:417–30.
21. Klein ME, Kovatcheva M, Davis LE, Tap WD, Koff A. CDK4/6 Inhibitors: the mechanism of action may not be as simple as once thought. Cancer Cell 2018;34:9–20.
22. Patnaik A, Rosen LS, Tolaney SM, Tolcher AW, Goldman JW, Gandhi L, et al. Efficacy and safety of abemaciclib, an inhibitor of CDK4 and CDK6, for patients with breast cancer, non-small cell lung cancer, and other solid tumors. Cancer Discov 2016;6:740–53.
23. Kosovec JE, Zaidi AH, Omstead AN, Matsui D, Biedka MJ, Cox EJ, et al. CDK4/6 dual inhibitor abemaciclib demonstrates compelling preclinical activity against esophageal adenocarcinoma: a novel therapeutic option for a deadly disease. Oncotarget 2017;8:100421–32.
24. Dowless MS, Lowery CD, Shackleford T, Renschler M, Stephens J, Flack R, et al. Abemaciclib is active in preclinical models of Ewing's sarcoma via multi-pronged regulation of cell cycle, DNA methylation, and interferon pathway signaling. Clin Cancer Res 2018;24:6028–39.
25. Golan T, Stossel C, Schvimer M, Atias D, Halperin S, Buzhor E, et al. Pancreatic cancer ascites xenograft-an expeditious model mirroring advanced therapeutic resistant disease. Oncotarget 2017; 8:40778–90.
26. Qiu W, Sahin F, Iacobuzio-Donahue CA, Garcia-Carracedo D, Wang WM, Kuo CY, et al. Disruption of p16 and activation of Kras in pancreas increase ductal adenocarcinoma formation and metastasis in vivo. Oncotarget 2011;2:862–73.
27. Hafner M, Niepel M, Chung M, Sorger PK. Growth rate inhibition metrics correct for confounders in measuring sensitivity to cancer drugs. Nat Methods 2016;13:521–7.
28. Lal S, Cheung EC, Zarei M, Preet R, Chand SN, Mambelli-Lisboa NC, et al. CRISPR Knockout of the HuR gene causes a xenograft lethal phenotype. Mol Cancer Res 2017;15:696–707.
29. Pineda DM, Rittenhouse DW, Valley CC, Cozzitorto JA, Burkhart RA, Leiby B, et al. HuR's post-transcriptional regulation of Death receptor 5 in pancreatic cancer cells. Cancer Biol Ther 2012;13:946–55.
30. Deer EL, González-Hernández J, Coursen JD, Shea JE, Ngatia J, Scaife CL, et al. Phenotype and genotype of pancreatic cancer cell lines. Pancreas 2010;39:425–35.
31. Huang L, Goodrow TL, Zhang SY, Klein-Szanto AJ, Chang H, Ruggeri BA, et al. Deletion and mutation analyses of the P16/MTS-1 tumor suppressor gene in human ductal pancreatic cancer reveals a higher frequency of abnormalities in tumor-derived cell lines than in primary ductal adenocarcinomas. Cancer Res 1996;56:1137–41.
32. Baughn LB, Di Liberto M, Wu K, Toogood PL, Louie T, Gottschalk R, et al. A novel orally active small molecule potently induces G1 arrest in primary myeloma cells and prevents tumor growth by specific inhibition of cyclin-dependent kinase 4/6. Cancer Res 2006;66:7661–7.
33. Chen JH, Stoeber K, Kingsbury S, Ozanne SE, Williams GH, Hales CN, et al. Loss of proliferative capacity and induction of senescence in oxidatively stressed human fibroblasts. J Biol Chem 2004;279: 49439–46.
34. Yoshizaki K, Fujiki T, Tsunematsu T, Yamashita M, Udono M, Shirahata S, et al. Pro-senescent effect of hydrogen peroxide on cancer cells and its possible application to tumor suppression. Biosci Biotechnol Biochem 2009;73:311–5.
35. Song Y, Baba T, Mukaida N. Gemcitabine induces cell senescence in human pancreatic cancer cell lines. Biochem Biophys Res Commun 2016;477: 515–9.
36. Jonchere B, Vétillard A, Toutain B, Lam D, Bernard AC, Henry C, et al. Irinotecan treatment and senescence failure promote the emergence of more transformed and invasive cells that depend on anti-apoptotic Mcl-1. Oncotarget 2015;6:409–26.
37. Altieri P, Murialdo R, Barisione C, Lazzarini E, Garibaldi S, Fabbi P, et al. 5-fluorouracil causes endothelial cell senescence: potential protective role of glucagon-like peptide 1. Br J Pharmacol 2017;174:3713–26.
38. Seignez C, Martin A, Rollet CE, Racoeur C, Scagliarini A, Jeannin JF, et al. Senescence of tumor cells induced by oxaliplatin increases the efficiency of a lipid A immunotherapy via the recruitment of neutrophils. Oncotarget 2014;5:11442–51.
39. Provinciali M, Cardelli M, Marchegiani F, Pierpaoli E. Impact of cellular senescence in aging and cancer. Curr Pharm Des 2013;19:1699–709.
40. Di Veroli GY, Fornari C, Wang D, Mollard S, Bramhall JL, Richards FM, et al. Combenefit: an interactive platform for the analysis and visualization of drug combinations. Bioinformatics 2016;32:2866–8.
41. Wu X, Lan L, Wilson DM, Marquez RT, Tsao WC, Gao P, et al. Identification and validation of novel small molecule disruptors of HuR-mRNA interaction. ACS Chem Biol 2015;10:1476–84.
42. Muralidharan R, Babu A, Amreddy N, Srivastava A, Chen A, Zhao YD, et al. Tumor-targeted nanoparticle delivery of HuR siRNA inhibits lung tumor growth in vitro and in vivo by disrupting the oncogenic activity of the RNA-binding protein HuR. Mol Cancer Ther 2017;16:1470–86.
43. Lin GL, Ting HJ, Tseng TC, Juang V, Lo YL. Modulation of the mRNA-binding protein HuR as a novel reversal mechanism of epirubicin-triggered multidrug resistance in colorectal cancer cells. PLoS One 2017;12: e0185625.
44. Guo J, Lv J, Chang S, Chen Z, Lu W, Xu C, et al. Inhibiting cytoplasmic accumulation of HuR synergizes genotoxic agents in urothelial carcinoma of the bladder. Oncotarget 2016;7:45249–62.
45. Rozengurt E, Sinnett-Smith J, Eibl G. Yes-associated protein (YAP) in pancreatic cancer: at the epicenter of a targetable signaling network associated with patient survival. Signal Transduct Target Ther 2018;3:11.
46. Zhang YH, Li B, Shen L, Shen Y, Chen XD. The role and clinical significance of YES-associated protein 1 in human osteosarcoma. Int J Immunopathol Pharmacol 2013;26:157–67.
47. Wen Y, Ji Y, Zhang Y, Jiang B, Tang C, Wang Q, et al. Knockdown of Yes-associated protein induces the apoptosis while inhibits the proliferation of human periodontal ligament stem cells through crosstalk between Erk and Bcl-2 signaling pathways. Int J Med Sci 2017;14:1231–40.
48. Li F, Xu Y, Liu B, Singh PK, Zhao W, Jin J, et al. YAP1-mediated CDK6 activation confers radiation resistance in esophageal cancer - rationale for the combination of YAP1 and CDK4/6 inhibitors in esophageal cancer. Clin Cancer Res 2018;25:2264–77.
49. Li Y, Wang S, Wei X, Zhang S, Song Z, Chen X, et al. Role of inhibitor of yes-associated protein 1 in triple-negative breast cancer with taxol-based chemoresistance. Cancer Sci 2018;110:561–7.
50. Tate SC, Burke TF, Hartman D, Kulanthaivel P, Beckmann RP, Cronier DM, et al. Optimising the combination dosing strategy of abemaciclib and vemurafenib in BRAF-mutated melanoma xenograft tumours. Br J Cancer 2016;114:669–79.
51. Goldstein D, El-Maraghi RH, Hammel P, Heinemann V, Kunzmann V, Sastre J, et al. nab-Paclitaxel plus gemcitabine for metastatic pancreatic cancer: long-term survival from a phase III trial. J Natl Cancer Inst 2015; 107:e325331.
52. Gelbert LM, El-Maraghi RH, Hammel P, Heinemann V, Kunzmann V, Sastre J, et al. Preclinical characterization of the CDK4/6 inhibitor LY2835219: in-vivo cell cycle-dependent/independent anti-tumor activities alone/in combination with gemcitabine. Invest New Drugs 2014;32: 825–37.